Available online at www.sciencedirect.com

SCIENCE DIRECT®

Nuclear Instruments and Methods in Physics Research B 247 (2006) 52–57

NIM B Beam Interactions with Materials & Atoms

www.elsevier.com/locate/nimb

Theory of ionization processes in positron–atom collisions

R. Della Picca [a], J. Fiol [a], R.O. Barrachina [a,*], V.D. Rodríguez [b]

[a] *Centro Atómico Bariloche and Instituto Balseiro[1], 8400 S.C. de Bariloche, Río Negro, Argentina*

[b] *Departamento de Física, Facultad de Ciencias Exactas y Naturales, Universidad de Buenos Aires, 1428 Buenos Aires, Argentina*

Available online 9 March 2006

Abstract

We review past and present theoretical developments in the description of ionization processes in positron–atom collisions. Starting from an analysis that incorporates all the interactions in the final state on an equal footing and keeps an exact account of the few-body kinematics, we perform a critical comparison of different approximations, and how they affect the evaluation of the ionization cross section. Finally, we describe the appearance of fingerprints of capture to the continuum, saddle-point and other kinematical mechanisms.

PACS: 34.10.+x; 34.50.Fa

Keywords: Ionization; Collision dynamics; Scattering; Electron spectra; Antimatter; Positron impact; Saddle-point electrons; Wannier; CDW

1. Introduction

The simple ionization collision of a hydrogenic atom by the impact of a structureless particle, the "three-body problem", is one of the oldest unsolved problems in physics. The two-body problem was analyzed by Johannes Kepler in 1609 and solved by Isaac Newton in 1687. The three-body problem, on the other hand, is much more complicated and cannot be solved analytically, except in some particular cases. In 1765, for instance, Leonhard Euler discovered a "collinear" solution in which three masses start in a line and remain lined-up. Some years later, Lagrange discovered the existence of five equilibrium points, known as the Lagrange points.

Even the most recent quests for solutions of the three-body scattering problem use similar mathematical tools and follow similar paths than those travelled by astronomers and mathematicians in the past three centuries. For instance, in the center-of-mass reference system, we describe the three-body problem by any of the three possible sets of the spatial coordinates already introduced by Jacobi in 1836. All these pairs are related by lineal point canonical transformations, as described in [1]. In momentum space, the system is described by the associated pairs ($\mathbf{k}_\mathrm{T}$,$\mathbf{K}_\mathrm{T}$), ($\mathbf{k}_\mathrm{P}$,$\mathbf{K}_\mathrm{P}$) and ($\mathbf{k}_\mathrm{N}$,$\mathbf{K}_\mathrm{N}$). Switching to the Laboratory reference frame, the final momenta of the electron of mass m, the (recoil) target fragment of mass M_T and the projectile of mass M_P can be written in terms of the Jacobi impulses $\mathbf{K}_\mathrm{j}$ by means of Galilean transformations [1]

$$\mathbf{k} = m\mathbf{v}_{CM} + \mathbf{K}_\mathrm{N}, \quad \mathbf{K} = M_\mathrm{P}\mathbf{v}_{CM} + \mathbf{K}_\mathrm{T} \text{ and}$$
$$\mathbf{K}_R = M_\mathrm{T}\mathbf{v}_{CM} - \mathbf{K}_\mathrm{P}.$$

For decades, the theoretical description of ionization processes has assumed simplifications of the three-body kinematics in the final state, based on the fact that

- in an ion–atom collision, one particle (the electron) is much lighter than the other two,
- in an electron–atom or positron–atom collision, one particle (the target nucleus) is much heavier than the other two.

For instance, based on what is known as Wick's argument, the overwhelming majority of the theoretical

* Corresponding author. Tel.: +54 2944 445192; fax: +54 2944 445149. *E-mail address:* barrachina@ib.edu.ar (R.O. Barrachina).

[1] Comisión Nacional de Energía Atómica (CNEA) and Universidad Nacional de Cuyo (UNC), Argentina.

0168-583X/$ - see front matter
doi:10.1016/j.nimb.2006.01.039

descriptions of ion–atom ionization collisions uses an impact-parameter approximation, where the projectile follows an undisturbed straight line trajectory throughout the collision process, and the target nucleus remains at rest [2]. It is clear that to assume that the projectile follows a straight line trajectory makes no sense in the theoretical description of electron or positron–atom collisions. However, it is usually assumed that the target nucleus remains motionless.

These simplifications of the problem were introduced in the eighteenth century. The unsolvable three-body problem was simplified, to the so-called restricted three-body problem, where one particle is assumed to have a mass small enough not to influence the motion of the other two particles. Though introduced as a means to provide approximate solutions to systems such as Sun–planet–comet within a Classical Mechanics framework, it has been widely used in atomic physics in the so-called impact-parameter approximation to ion–atom ionization collisions.

Another simplification of the three-body problem widely employed in the nineteenth century assumes that one of the particles is much more massive than the other two and remains in the center of mass unperturbed by the other two. This approximation has been widely used in electron–atom or positron–atom ionization collisions.

2. The multiple differential cross section

A kinematically complete description of a three-body continuum final-state in any atomic collision would require, in principle, the knowledge of nine variables, such as the components of the momenta associated to each of the three particles in the final state. However, the condition of momentum and energy conservation reduces this number to five. Furthermore, whenever the initial targets are not prepared in any preferential direction, the multiple differential cross section has to be symmetric by a rotation of the three-body system around the initial direction of motion of the projectile. Thus, leaving aside the internal structure of the three fragments in the final state, only four out of nine variables are necessary to completely describe the scattering process. Therefore, a complete characterization of the ionization process may be obtained with a quadruple differential cross section:

$$\frac{\mathrm{d}\sigma}{\mathrm{d}q_1\mathrm{d}q_2\mathrm{d}q_3\mathrm{d}q_4}.$$

There are many possible sets of four variables to use. For, instance, we can chose azimuthal angles of the electron and of one of the other two particles, the relative angle between the planes of motion, and the energy of one particle.

$$\frac{\mathrm{d}\sigma}{\mathrm{d}E_1\mathrm{d}\cos\theta_1\mathrm{d}\cos\theta_2\mathrm{d}\phi}.$$

Such a choice is arbitrary, but complete in the sense that any other set of variables can be related to this one. A similar choice of independent variables has been standard for the description of atomic ionization by electron impact, both theoretically and experimentally [3,4].

A picture of the very general quadruple differential cross section is not feasible. Thus, it is usually necessary to reduce the number of variables in the cross section. This can be achieved by fixing one or two of them at certain particular values or conditions. For instance, we might arbitrarily restrict ourselves to describe a coplanar (i.e. $\phi = 0$) or a collinear motion (i.e. $\phi = 0$ and $\theta_1 = \theta_2$), so as to reduce the dependence of the problem to three or two independent variables, respectively.

The other option is to integrate the quadruple differential cross section over one or more variables.

$$\frac{\mathrm{d}\sigma}{\mathrm{d}q_1\mathrm{d}q_2\mathrm{d}q_3} = \int \frac{\mathrm{d}\sigma}{\mathrm{d}q_1\mathrm{d}q_2\mathrm{d}q_3\mathrm{d}q_4}\mathrm{d}q_4.$$

The former has been widely used to study electron–atom collisions, while the latter has been the main tool to characterize ion–atom and positron–atom ionization collisions. Particularly important has been the use of single particle spectroscopy, where the momentum of one of the particles is measured.

3. Single particle momentum distributions

In ionization by positron impact it is feasible to study the momentum distribution of any of the involved fragments. As is shown in Fig. 1, the momentum distributions for the emitted electron and the positron present several structures. First, we can observe a threshold at high electron or positron velocities because there is a limit in the kinetic energy that any particle can absorb from the system. The second structure is a ridge set along a circle. It corresponds to a binary collision of the positron with the emitted electron, with the target nucleus playing practically no role. Finally, there is a cusp and an anticusp at zero velocity in the electron and positron momentum distributions, respectively. The first one corresponds to the excitation of the electron to a low-energy continuum state of the target. The second is a depletion due to the impossibility of capture of the positron by the target nucleus. These momentum distributions allow us to study the main characteristics of ionization collisions. However, we have to keep in mind that any experimental technique that analyzes only one of the particles in the final-state can only provide a partial insight into the ionization processes. The quadruple differential cross sections might display collision properties that are washed out by integration in this kind of experiments.

4. Theoretical model

The main question that we want to address in this communication is if there are some important collision

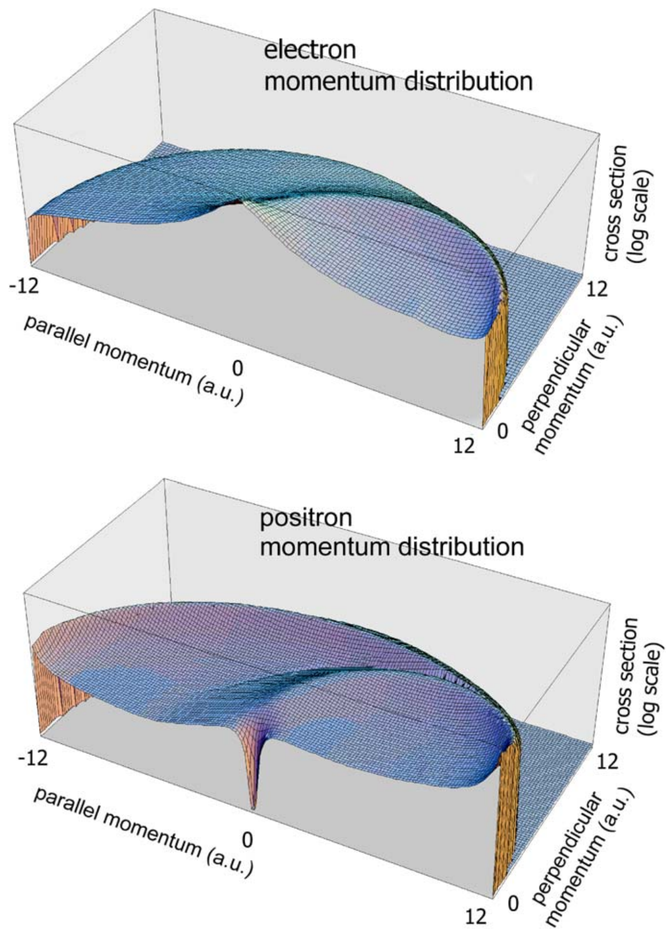

Fig. 1. Electron and positron momentum distributions for the ionization of helium by impact of positrons with incident velocity $v = 12$ a.u.

properties in positron–atom collisions, that are not observable in total, single or double differential ionization cross sections, and that therefore have not yet been discovered. In order to understand the origin of these structures, we compare the corresponding cross sections with those obtained in ion–atom collisions. To fulfill this objective it is necessary to have a full quantum-mechanical treatment able to deal simultaneously with ionization collisions by impact of both heavy and light projectiles that is therefore equally applicable – for instance – to ion–atom or positron–atom collisions. A theory with this characteristics will allow us to study the changes of any given feature of multiple-differential cross-sections when the mass relations among the fragments vary. In particular, it would allow us to study the variation when changing between the two restricted kinematical situations.

The second important point is to treat all the interactions in the final state on an equal footing. As we have just explained, in ion–atom collisions, the internuclear interaction plays practically no role in the momentum distribution of the emitted electron and has therefore not been considered in the corresponding calculation. In this work, this kind of assumption has been avoided.

The cross section of interest within this framework is

$$\frac{d\sigma}{dE_e d\Omega_k d\Omega_K} = \frac{(2\pi)^4}{v} |t_{if}(\mathbf{k}, \mathbf{K})|^2 \frac{k m_N K^2}{\left| K + m_N \widehat{K} \cdot (\mathbf{k} - \mathbf{v})/M_T \right|}.$$

The transition matrix can be alternatively written in *post* or *prior* forms as

$$t_{if} = \langle \Psi_f^- | V_i | \Psi_i \rangle, \quad t_{if} = \langle \Psi_f | V_f | \Psi_i^- \rangle,$$

where the perturbation potentials are defined by $(H - E)\Psi_i = V_i\ \Psi_i$ and $(H - E)\Psi_f = V_f \Psi_f$.

For the Born-type initial state

$$\Psi_i(\mathbf{r}_T, \mathbf{R}_T) = \frac{e^{i\mathbf{K}_T \cdot \mathbf{R}_T}}{(2\pi)^{3/2}} \phi_i(\mathbf{r}_T),$$

which includes the free motion of the projectile and the initial bound state Φ_i of the target, and the perturbation potential V_i is simply the sum of the positron–electron and positron–nucleus interactions. The transition matrix may then be decomposed into two terms

$$t_{if} = \langle \Psi_f^- | V_i | \Psi_i \rangle = \left\langle \Psi_f^- \left| \frac{Z_T}{r_N} \right| \Psi_i \right\rangle + \left\langle \Psi_f^- \left| \frac{-1}{r_P} \right| \Psi_i \right\rangle$$
$$= t_N + t_P,$$

depending on whether the positron interacts first with the target nucleus or the electron.

In order to be consistent with our full treatment of the kinematics, it is necessary to describe the final state Ψ_f^- by means of a wavefunction that considers all the interactions on the same footing. Thus, we resort to a correlated C3 wave function

$$\Psi_f^{\pm} = \frac{e^{i(\mathbf{k}_T \cdot \mathbf{r}_T + \mathbf{K}_T \cdot \mathbf{R}_T)}}{(2\pi)^3} D_N^{\pm} D_P^{\pm} D_T^{\pm}$$

that includes distortions $D_j^{\pm}$ for the three active interactions. The final-channel perturbation potential for this choice of continuum wave function is [5]

$$V_f = \frac{\mathbf{K}_P \mathbf{K}_N}{M_P} - \frac{\mathbf{K}_T \mathbf{K}_N}{M_T} - \frac{\mathbf{K}_T \mathbf{K}_P}{m}, \quad \mathbf{K}_j = \frac{\nabla D_j^{-*}}{D_j^{-*}}. \tag{1}$$

In the case of pure coulomb potentials, the distortions are given by

$$D_j^{-*} \equiv D^{\pm}(v_j, \mathbf{k}_j, \mathbf{r}_j)$$
$$= \Gamma(1 \pm i v_j) e_1^{-\pi v_j/2} F_1(\mp i v_j; 1; -i(\mathbf{k}_j \mathbf{r}_j \mp k_j r_j)),$$

with $v_j = m_j Z_j / k_j$. This model was proposed by Garibotti and Miraglia [6] for ion–atom collisions, and by Brauner and Briggs six years later for positron–atom and electron–atom collisions [7]. However, in all these cases the kinematics of the problem was simplified, as discussed in the previous section, on the basis of the large asymmetry between the masses of the fragments involved. In addition, Garibotti and Miraglia neglected the matrix element of the interaction potential between the incoming projectile and the target ion, and made a peaking approximation to evaluate the transition matrix element. This further approximation was removed in a paper by Berakdar et al. (1992), although they kept the mass restrictions in their ion-impact ionization analysis.

5. The electron capture to the continuum cusp

Let us review some results in a collinear geometry. We choose as the two independent parameters the emitted electron momentum components, parallel and perpendicular to the initial direction of motion of the positron projectile. The energy of the projectile is 1 keV. In Fig. 2, we observe three different structures: two minima and a ridge.

The origin of the ridge is very well understood. It corresponds to the electron capture to the continuum (ECC) cusp discovered in ion–atom collisions three decades ago by Crooks and Rudd [8]. They measured the electron energy spectra in the forward direction and observed a cusp-shape peak at exactly the projectile's velocity. The first theoretical explanation [9] showed that it diverges in the same way as $1/k$. This cusp structure was the focus of a large amount of experimental and theoretical research.

Since the ECC cusp is an extrapolation across the ionization limit of capture into highly excited bound states, this same effect has to be present in positron–atom collisions. In fact, the observation of such an effect associated with positronium formation, while predicted two decades ago by Brauner and Briggs, remained a controversial issue. The reason for this dispute was that, in contrast to the case of ions, the positron outgoing velocity is not similar to that of impact, but is largely spread in angle and magnitude. Thus there is no particular velocity where to look for the cusp. And this is certainly so. If we evaluate the double differential cross section, we see that the cusp is clearly visible in ion–atom collisions, but just a very mild and spread shoulder in positron–atom collisions. Thus, to observe this structure it is necessary to increase the dimension of the cross section. For instance by considering a zero degree cut of the quadruple differential cross section in collinear geometry.

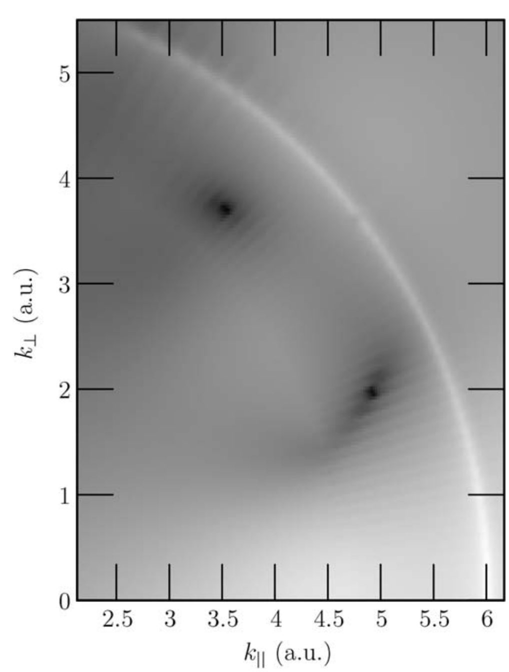

Fig. 2. QDCS for ionization of H_2 by impact of 1 keV positrons for emission of electrons in the direction of the projectile deflection.

Kover and Laricchia measured in 1998 the $d\sigma/dE_e d\Omega_k d\Omega_K$ cross section in a collinear condition at zero degree, for the ionization of H_2 molecules by 100 keV positron impact [10]. The structure is not so sharply defined as for impact observed for heavy ions because of the convolution that accounts for the experimental window in the positron and electron detection. Since the target recoil plays no significant role in this experimental situation, the present general theory gives results similar to those obtained by Berakdar [11], and both closely follow the experimental values.

The same kind of experiment was performed by Sarkadi and coworkers in Argon ionization by 75 keV proton impact. They measured the quadruple differential ionization cross section in a collinear geometry for ion–atom collisions for the first time, and found the ECC cusp as in positron impact at large angles. In this case, we have to keep a complete account of the kinematics in order to reproduce the experimental results [12].

6. Thomas mechanism

Let us now go back to the ionization of H_2 by 1 keV positron impact. A structure at 45° can be observed, which was predicted and explained in 1993 by Brauner and Briggs as due to the interference of two equivalent double-collision mechanisms. Each of these processes consists of a positron–electron binary collision, followed by the deflection by 90° of one of the light particles by the heavy nucleus. This mechanism was proposed by Thomas [13] as the main responsible of electron capture by fast heavy ions. In this case, since the electron and positron masses are equal, these two processes interfere at 45°.

If we lower the energy from 1000 eV to 100 eV, this structure at 45° disappears, a result that is consistent with the idea that the Thomas mechanism is a high energy effect. But there is another structure, at about 22.5°, that persists. We will consider this structure in the next section.

7. Saddle-point mechanism

The origin of the structure at about 22.5° is certainly more difficult to identify. To our best knowledge, it has not been predicted before in positron–atom collisions, even though the mechanism responsible of its origin was already been proposed in ion–atom collisions almost two decades before. The idea was that an electron could emerge from an ion–atom collision by lying in the saddle-point of the projectile and the residual target-ion potentials. This mechanism is clearly related to one of the equilibrium points discovered by Lagrange in 1772, or to the mechanism proposed by Wannier for low-energy electron emission. In the case of ion–atom collisions, the search for theoretical and experimental evidence of this mechanism was overcast by vivid controversy [14–18].

In the case of positron–atom collisions, for the electrons to be trapped in the saddle of the positron and residual-ion potentials, the electron and the positron must first perform a binary collision so as to end up with the right velocities

$$v_e = \sqrt{\frac{v^2 - 2|\varepsilon_i|}{1 + (1 + 1/\sqrt{Z_T})^2}} \quad \text{and}$$
$$v_P = \sqrt{\frac{v^2 - 2|\varepsilon_i|}{1 + 1/(1 + 1/\sqrt{Z_T})^2}}, \tag{2}$$

where ε_i is the binding energy of the target in the initial state.

Application of energy and momentum conservation principles shows that the positron is deviated in an angle

$$\theta_P = \arccos\left[\frac{v_P}{v}\left(1 + \frac{|\varepsilon_i|}{v_P^2}\right)\right]. \tag{3}$$

Finally, for the electron to emerge in the same direction as the positron, it must suffer a subsequent collision with the residual-nucleus in a Thomas-like process. In this second collision, the electron is deflected by 90° and the residual target ion recoils in a direction that forms an angle of about 135° with the electron and the positron. This mechanism is depicted in Fig. 4.

Thus, to check that the proposal of a saddle-point is correct, we look at whether our calculations show structures that are consistent with this description of saddle-point electron production.

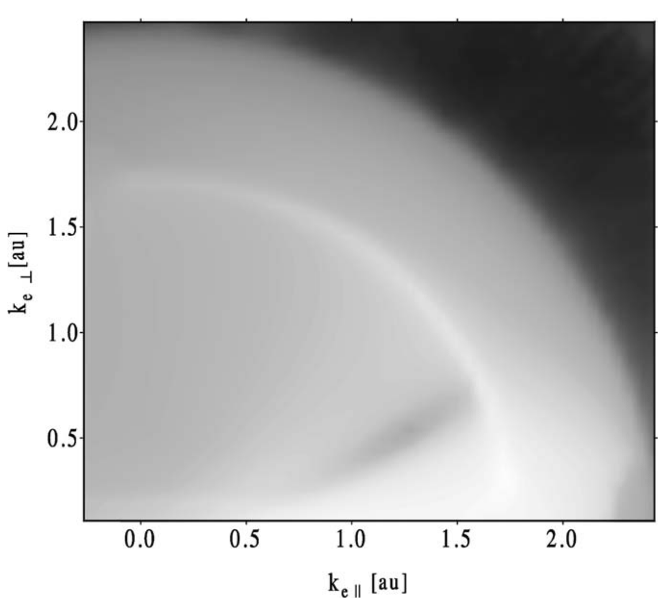

Fig. 3. QDCS for H_2 ionization by 100 eV positrons in the restricted collinear geometry.

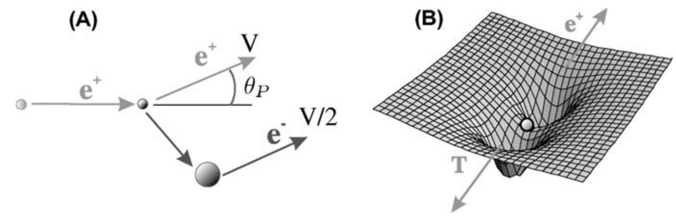

Fig. 4. Mechanism proposed to lead to the observed saddle-like structure.

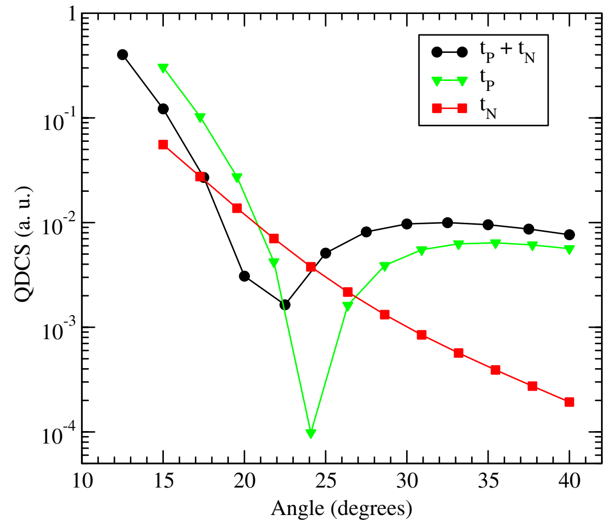

Fig. 5. QDCS for ionization of H_2 by impact of positrons at 100 eV and electron energy $E_e = 19$ eV.

The minimum observed in the QDCS of Figs. 3 and 4 are located at precisely those points where the previous conditions on the energy and angle of any of the three particles are met.

We made another test on the validity of the saddle-point mechanism. Fig. 5 shows that the structure arises exclusively from the t_P term. This result is consistent with the proposed mechanism, where the saddle-point structure arises from a first positron–electron collision. Afterwards, both positron and electron are scattered by the nucleus.

8. Conclusions

Summarizing the results presented in this communication, we have investigated the ionization of molecular hydrogen by the impact of positrons. The obtained quadruple differential cross-sections for the electron and the positron emerging in the same direction show three dominant structures. One is the well-known electron capture to the continuum peak. Another one is the Thomas mechanism. Finally, there is a minimum that might be interpreted as due to the so-called "saddle-point" ionization mechanism.

But the main conclusion is that the study of the fully differential cross section might be hindered by a great number of difficulties, but the reward is that many different structures can be observed that otherwise are missed in double, single differential or total cross sections.

References

[1] J. Fiol, R.O. Barrachina, V.D. Rodríguez, J. Phys. B: At. Mol. Opt. Phys. 35 (1) (2002) 149.
[2] N. Stolterfoht, R.D. Dubois, R.D. Rivarola, Electron Emission in Heavy Ion–Atom Collisions, Springer Series on Atoms and Plasmas, Springer, Berlin, 1997.
[3] H. Ehrhardt, G. Knoth, P. Schlemmer, K. Jung, Phys. Lett. A 110 (1985) 92.
[4] A. Lahmam-Bennani, J. Phys. B: At. Mol. Opt. Phys. 24 (10) (1991) 2401.
[5] J. Fiol, R.E. Olson, Nucl. Instr. and Meth. B 205 (2003) 474.
[6] C.R. Garibotti, J.E. Miraglia, Phys. Rev. A 21 (1980) 572.
[7] M. Brauner, J.S. Briggs, J. Phys. B: At. Mol. Opt. Phys. 19 (1986) L325.
[8] G.B. Crooks, M.E. Rudd, Phys. Rev. Lett. 25 (1970) 1599.
[9] J.H. Macek, Phys. Rev. A 1 (1970) 235.
[10] Á. Kövér, G. Laricchia, Phys. Rev. Lett. 80 (1988) 5309.
[11] J. Berakdar, Phys. Rev. Lett. 81 (1998) 1393.
[12] J. Fiol, V.D. Rodríguez, R.O. Barrachina, J. Phys. B: At. Mol. Opt. Phys. 34 (5) (2001) 933.
[13] L.H. Thomas, Proc. R. Soc. A 114 (1927) 561.
[14] T.G. Winter, C.D. Lin, Phys. Rev. A 29 (1984) 3071.
[15] R.E. Olson, T.J. Gay, H.G. Berry, E.B. Hale, V.D. Irby, Phys. Rev. Lett. 59 (1987) 36.
[16] G. Bandarage, R. Parson, Phys. Rev. A 41 (1990) 5878.
[17] E.Y. Sidky, C. Illescas, C.D. Lin, J. Phys. B: At. Mol. Opt. Phys. 34 (6) (2001) L163.
[18] L. Ponce, R. Taïeb, V. Véniard, A. Maquet, J. Phys. B: At. Mol. Opt. Phys. 37 (15) (2004) L297.